

Rec'd PCT/PTO 15 JUN 2005

PATENT
Atty Docket No. 102364
Express Mail Label No. EV 535074245 US

UNITED STATES PATENT AND TRADEMARK OFFICE

Applicant(s):	Tomasz Heyduk, et al.	Group No.:	To Be Assigned
Serial No.:	To Be Assigned	Examiner:	To Be Assigned
Filing Date:	June 15, 2005	Conf. No.:	To Be Assigned
For:	BIOSENSORS FOR DETECTING MACROMOLECULES AND OTHER ANALYTES		

Mail Stop: PCT
Commissioner for Patents
P.O. Box 1450
Alexandria, VA 22313-1450

**PETITION UNDER 37 CFR 1.84(b)(2)
FOR ACCEPTANCE OF COLOR PHOTOGRAPHS**

Dear Sir:

Applicants hereby request that the color photographs be accepted in the referenced utility patent application pursuant to 37 CFR 1.84(b)(2). Accordingly, please find the following enclosed items as required by 37 CFR 1.84:

- (i) Three (3) sets of color photographs of Figs. 1-33 and,
- (ii) One (1) complete set of black & white photocopies of Figs. 1-33, accurately depicting the subject matter shown in the color photographs.

The referenced color photographs are as follows:

06/21/2005 LLANDGRA 00000080 10539107

05 FC:1464

130.00 OP

CERTIFICATE OF MAILING

I hereby certify that, on the date shown below, this correspondence is being

deposited with the United States Postal Service in an envelope addressed to Mail Stop: PCT, Commissioner for Patents, P.O. Box 1450, Arlington, VA 22313-1450.

MAILING

37 C.F.R. §1.8
 as first class mail.

37 C.F.R. §1.10
 as "Express Mail Post Office to Addressee"
EXPRESS MAIL NO. EV 535074245 US.

FACSIMILE TRANSMISSION

transmitted by facsimile to the Patent and Trademark Office.

M. Sue Clements
Name of Depositor

M. Sue Clements
Signature

6-15-05

Date

Fig. 1. Overall design of molecular beacons for detecting proteins. (A) Variant of the design for targets lacking natural DNA binding activity. The beacon in this case will be composed of two aptamers developed to recognize two different epitopes of the protein. (B) Variant of the design for target exhibiting natural DNA binding activity. The beacon in this case will be composed of a short double-stranded DNA fragment containing the DNA sequence corresponding to the DNA-binding site and DNA (RNA) aptamer developed to recognize a different epitope of the protein.

Fig. 2. Methods for preparing aptamers to be used in molecular biosensors. (A) Selection of an aptamer in the presence of a known aptamer construct. The in vitro evolution process is initiated with a nucleic acid construct, an aptamer construct (composed of an known aptamer (red), a linker, and a short oligonucleotide sequence (blue)), and the target (gray). The blue color bars depict complementary short oligonucleotide sequences. (B) Simultaneous selection of two aptamers that bind distinct epitopes of the same target (gray). The in vitro evolution process is initiated with two types of nucleic acid constructs (the primer1-2 construct and the primer3-4 construct) and the target. The blue color bar depicts short complementary sequences at the end of the two types of nucleic acid constructs. (C) Alternative design for simultaneous selection of two aptamers that bind distinct epitopes of the same target (gray). An additional pair of short oligonucleotides (blue bars) connected by a flexible linker is present during the selection process. These oligonucleotides will be complementary to short oligonucleotide sequences at the end of the nucleic acid constructs (in primer 1 and primer 4). Their presence during selection will provide a bias towards selecting pairs of aptamers capable of simultaneously binding to the target. Before cloning of the selected nucleic acid constructs the pairs of selected sequences will

be ligated to preserve the information regarding the preferred pairs between various selected constructs. (D) Selection of an aptamer in the presence of a known antibody construct. The in vitro evolution process is initiated with a nucleic acid construct, an antibody construct (composed of an known antibody (red), a linker, and a short oligonucleotide sequence (blue)), and the target (gray). The blue color bars depict complementary short oligonucleotide sequences. (E) Selection of an aptamer in the presence of a known double-stranded DNA construct. The in vitro evolution process is initiated with a nucleic acid construct, an aptamer construct (composed of an known double-stranded DNA sequence (red), a linker, and a short oligonucleotide sequence (blue)), and the target (gray). The blue color bars depict complementary short oligonucleotide sequences.

Fig. 3. Comparison of the design of molecular beacons for DNA binding proteins (A) and molecular beacons for detecting proteins based on aptamers directed to two different epitopes of the protein (B).

Fig. 4. Aptamer constructs containing aptamers binding thrombin at fibrinogen exosite (60-18 [29]) and at heparin exosite (G15D).

Fig. 5. Binding of fluorescein-labeled aptamers to thrombin. (A) Binding of 60-18 [29] aptamer (THR1) (50 nM) detected by fluorescence polarization; (B) Binding of G15D aptamer (THR2) (50 nM) detected by change in fluorescence intensity; (C) Quantitative equilibrium titration of fluorescein-labeled G15D aptamer (THR2) (20 nM) with thrombin. Solid line represents nonlinear fit of experimental data to an equation describing formation of 1:1 complex between the aptamer and thrombin; (D) Quantitative equilibrium titration of fluorescein-labeled G15D aptamer (THR2) (20 nM) with thrombin in the presence of ten fold excess of unlabeled

60-18 [29] aptamer (THR3). Solid line represents nonlinear fit of experimental data to an equation describing formation of 1:1 complex between the aptamer and thrombin

Fig. 6. Illustration of the competition between thrombin aptamer constructs and fluorescein-labeled G15D aptamer (THR2) for binding to thrombin. Fluorescence spectra of 50 nM fluorescein-labeled G15D (THR2) with and without thrombin in the absence of competitor (A), in the presence of 150 nM THR3 (B), in the presence of 150 nM THR4 (C), and in the presence of 150 nM THR7 (D).

Fig. 7. Summary of experiments probing competition between thrombin aptamer constructs and fluorescein-labeled G15D aptamer (THR2) for binding to thrombin. Fluorescence intensity of fluorescein-labeled G15D aptamer (THR2) (50 nM) in the absence and the presence of the competitor (250 nM) was used to determine % of THR2 bound in the presence of the competitor. Thrombin concentration was 75 nM. The values of dissociation constants shown in the figure were calculated from a separate experiment in which 200 nM fluorescein-labeled G15D aptamer (THR2), 200 nM competitor and 150 nM thrombin were used.

Fig. 8. The effect of 60-18 [29] aptamer (THR3) on the competition between fluorescein-labeled G15D aptamer (THR2) and THR5 construct for binding to thrombin. Fluorescence spectra of 200 nM fluorescein-labeled G15D (THR2) with and without thrombin (150 nM) in the absence of the competitor (A), in the presence of 1000 nM THR3 and 200 nM THR5 (B), in the presence of 1000 nM THR3 (C), and in the presence of 200 nM THR5 (D).

Fig. 9. Binding of THR7 aptamer construct to thrombin detected by gel electrophoresis mobility shift assay. Samples of 417 nM THR7 were incubated with various amounts of

thrombin (0 to 833 nM) and after 15 min incubation were loaded on a native 10% polyacrylamide gel. (A) Image of the gel stained with Sybr Green. (B) Intensity of the band corresponding to THR7-thrombin complex as a function of thrombin concentration

Fig. 10. Family of bivalent thrombin aptamer constructs in which G15D and 60-18 [29] aptamers were connected to a 20 bp DNA duplex by a 9-27 nt long poly T linker.

Fig. 11. Binding of thrombin to bivalent aptamer constructs (33 nM each) illustrated in Fig. 8 detected by electrophoretic mobility shift assay (EMSA). Asterisk marks the lane best illustrating preferential binding of thrombin to constructs with 27 and 17 nt poly T linker over the constructs with 9 nt poly T linker. Thrombin concentration was varied from 0 to 400 nM.

Fig. 12. Thrombin beacon design using G15D and 60-18 [29] aptamers connected to 9 bp fluorophore (or quencher)-labeled “signaling” duplex through 17 nt poly T linker. (A) Nucleotide sequence of the fluorescein-labeled G15D construct (THR9) and dabcyl-labeled 60-18 [29] construct (THR8). (B) Mechanism of signaling by thrombin beacon. (C) Fluorescence signal change detected upon addition of thrombin to the thrombin beacon. For comparison, titration of the fluorescein-labeled G15D construct (THR9) with thrombin in the absence of dabcyl-labeled 60-18 [29] construct (THR8) is also shown (donor only curve).

Fig. 13. A thrombin beacon design. G15D and 60-18 [29] aptamers were connected to 7 bp fluorophore (or quencher)-labeled “signaling” duplex through a linker containing 5 Spacer18 units. (A) Nucleotide sequence of the fluorescein-labeled G15D construct (THR21) and dabcyl-labeled 60-18 [29] construct (THR20). X corresponds to Spacer 18 moiety. (B) Mechanism of signaling by thrombin beacon. (C) Fluorescence signal change detected upon addition of

thrombin to the thrombin beacon. For comparison, titration of the fluorescein-labeled G15D construct (THR21) with thrombin in the absence of dabcyl-labeled 60-18 [29] construct (THR20) is also shown (donor only curve). Signal change (%) was calculated as $100^* (I_0 - I) / I_0$ where I and I_0 correspond to dilution-corrected fluorescence emission intensity observed in the presence and absence of a given thrombin concentration, respectively. Inset shows fluorescence emission spectra recorded at various concentrations of thrombin corresponding to data points in the main graph.

Fig. 14. Binding of thrombin to the beacon illustrated in Fig. 13 (THR20/THR21) detected by gel electrophoresis mobility shift assay. The gel was imaged for fluorescein emission (i.e. only THR21 component of the beacon is visible).

Fig. 15. (A) Sensitivity of thrombin detection at two different concentrations of the beacon. Red circles: 50 nM THR21 and 95 nM THR20. Blue circles: 5 nM THR21 and 9.5 nM THR20. (B) Specificity of the beacon for thrombin. 50 nM THR21 and 95 nM THR20 were titrated with thrombin (red circles) and trypsin (blue circles).

Fig. 16. Reversal of thrombin beacon signal by competitor aptamer constructs. Fluorescence intensity of 50 nM THR21, 95 nM THR20, and 100 nM thrombin was measured at increasing concentrations of competitor DNA's. The data are plotted as a relative fluorescence increase with respect to a signal (F_0) of a starting beacon and thrombin mixture. Open blue squares: THR7; filled black circles: THR14/THR15; filled red squares: THR16/THR17; filled blue triangles: THR18/THR19; open magenta triangles: THR3; green filled inverted triangles: THR4; open black triangles: nonspecific single stranded DNA.

Fig. 17 The binding of aptamer constructs to thrombin. (A) Binding of G15D aptamer (THR2) (50 nM) detected by change in fluorescence intensity of 5' fluorescein moiety. Solid line represents the best fit of the experimental data to a simple 1:1 binding isotherm. (B) Binding of G15D aptamer (THR2) in the presence of 10x excess of unlabeled 60-18 [29] aptamer. Solid line represents the best fit of the experimental data to a simple 1:1 binding isotherm. (C) Summary of experiments probing competition between thrombin aptamer constructs and fluorescein-labeled G15D aptamer (THR2). Fluorescence intensity of THR2 (200 nM) was used to determine % THR2 bound in the presence of competitor (200 nM). Thrombin was 150 nM. The labels above each bar indicate relative affinity (expressed as fold increase of affinity constant) of the competitor compared to the affinity of THR2 aptamer. (D) Binding of THR7 aptamer construct to thrombin detected by gel electrophoresis mobility shift assay. Intensity of the band corresponding to THR7-thrombin complex is plotted as a function of thrombin concentration. Inset: Image of the gel stained with Sybr Green. Fluorescence change (%) was calculated as $100^* \frac{(I-I_0)}{I_0}$ where I and I_0 correspond to dilution-corrected fluorescence emission intensity observed in the presence and absence of a given thrombin concentration, respectively.

Fig. 18 Variants of thrombin beacon with various combinations of donor-acceptor fluorophores. (A) fluorescein-dabcyl; (B) fluorescein-Texas Red; (C) fluorescein-Cy5, (D) Cy3-Cy5. Emission spectra of the beacon in the absence (black line) and presence (red line) of thrombin are shown. Insets show false color images of microplate wells containing corresponding beacon and indicated concentrations of thrombin. The images were obtained on Bio-Rad Molecular Imager FX using the following excitation-emission settings: (A) 488 nm laser – 530 nm bandpass filter; (B) 488 nm laser – 640 nm bandpass filter; (C) 488 nm laser –

695 nm bandpass filter; (D) 532 nm laser – 695 nm bandpass filter. Fluorescence is in arbitrary units (corrected for instrument response) and is plotted in a linear scale.

Fig. 19 Response curves for the beacon with various combinations of donor-acceptor pairs. (A) fluorescein-dabcyl, (B) fluorescein-Texas Red, (C) Cy3-Cy5, (D) fluorescein-Cy5, (E) europium chelate-Cy5, (F) Fold signal change observed for indicated donor-acceptor pair at saturating thrombin concentration. Insets show expanded view of data points at low thrombin concentrations. In all experiments 5 nM donor-labeled and 5.5 nM acceptor-labeled aptamer constructs were used. Signal change (fold) was calculated as I/I_0 where I and I_0 correspond to dilution-corrected acceptor fluorescence emission intensity (measured with donor excitation) observed in the presence and absence of a given thrombin concentration, respectively. Buffer background was subtracted from I and I_0 before calculating signal change.

Fig. 20 The dependence of the sensitivity of the thrombin beacon on a donor-acceptor pair. Response of 10 nM donor-labeled and 11 nM acceptor-labeled beacon was determined at low thrombin concentrations using beacon labeled with fluorescein-dabcyl pair (triangles), fluorescein-Texas Red pair (inverted triangles), and fluorescein-Cy5 pair (circles). Averages and standard deviations of four independent experiments are shown.

Fig. 21 The reproducibility and stability of thrombin beacon. (A) Five independent determinations of beacon signal at four different thrombin concentrations were performed. Data shown represent mean +/- standard deviation. (B) Thrombin beacon signal at four thrombin concentrations was monitored over time up to 24 hours. Data shown represent mean +/- standard deviation of 5 independent measurements. Beacon containing 5 nM fluorescein-labeled aptamer (THR21) and 5.5 nM Texas Red-labeled aptamer (THR27) was used in this experiment.

Fig. 22 shows the determination of Z'-factor for thrombin beacon. Panel in the middle of the plot shows the false color image of wells of the microplate corresponding to the experiment shown in a graph (the upper half of wells are + thrombin, the lower half of the wells is – thrombin. Beacon containing with 5 nM fluorescein-labeled aptamer (THR21) and 5.5 nM Texas Red-labeled aptamer (THR27) was used in this experiment. Signal corresponds to a ratio of acceptor to donor emission (in arbitrary units) measured with donor excitation.

Fig. 23 The detection of thrombin in complex mixtures. (A) Response of thrombin beacon at 1 nM thrombin concentration in the absence and presence of the excess of unrelated proteins. The data shown are averages and standard deviation of 4 independent experiments. (B) Detection of thrombin in HeLa extract “spiked” with various amounts of thrombin. Data shown are averages and standard deviation from 3 independent measurements. Concentrations of thrombin in cell extract were: 1.88 nM (green bars); 3.75 nM (pink bars); 7.5 nM (red bars). Signal for beacon mixture alone was ~ 25% lower than when cell extract (no thrombin added) was present (not shown) which was essentially the same as the signal observed in the presence of cell extract and specific competitor. (C) Time course of prothrombin to thrombin conversion catalyzed by Factor Xa monitored by thrombin beacon. (D) Detection of thrombin in plasma. Data shown are averages and standard deviation from 4 independent measurements. The volumes of plasma used (per 20 μ l assay mixture) were: 0.005 μ l (green bars); 0.015 μ l (red bars); 0.045 μ l (blue bars). “Specific” refers to unlabeled thrombin aptamer competitor (THR7) whereas “nonspecific” refers to random sequence 30 nt DNA. Signal in panels A, B and D corresponds to a ratio of acceptor to donor emission measured with donor excitation. Signals were normalized to value of 1 for beacon mixture alone (panels A and D) and beacon mixture in

the presence of cell extract (panel B). Panel C shows raw acceptor fluorescence intensity (with donor excitation).

Fig. 24 Various formations of molecular biosensors.

Fig. 25 The experimental demonstration of sensor design shown in Fig. 24F. (A) Principle of sensor function. (B) Increase of sensitized acceptor fluorescence upon titration of increasing concentrations of DNA binding protein to the mixture of donor and acceptor labeled sensor components.

Fig. 26 The experimental demonstration of a functioning sensor design shown in Fig. 24G. (A) Principle of sensor function. (B) Increase of sensitized acceptor fluorescence (emission spectrum labeled with "+") upon addition of single-stranded DNA containing two distinct sequence elements complementary to sensor elements to the mixture of two donor and acceptor labeled sensor components (spectrum labeled with "-").

Fig. 27 The experimental demonstration of the increased specificity of our sensor design compared to assays based on a single, target macromolecule-recognizing element.

Fig. 28 summarizes the selection of an aptamer that binds to thrombin at an epitope distinct from the binding site of the G15D aptamer. (A) An illustration of the reagents used to begin the process of selection. (B) The graph indicates the increase in thrombin binding with successive rounds of selection. (C) The sequences represent aptamers developed after 12 rounds of selection.

Fig. 29 The demonstration of the functional thrombin sensor comprising Texas Red-labeled THR27 and fluorescein-labeled THR35 or THR36 (both contain the sequence corresponding to that of clones 20, 21, 24, and 26 of Figure 5C). The fluorescence image represents the specificity of either 20nM (panel A) or 100nM (panel B) of the indicated biosensor.

Fig. 30 summarizes the simultaneous selection of two aptamers that bind to thrombin at distinct epitopes. (A) An illustration of the reagents used to begin the process of selection. (B) The graph indicates the increase in thrombin binding with successive rounds of selection. (C) The sequences represent aptamers developed after 13 rounds of selection.

Fig. 31 summarizes the selection of an aptamer that binds to CRP at an epitope distinct from the DNA-binding site. (A) An illustration of the reagents used to begin the process of selection. (B) The graph indicates the increase in thrombin binding with successive rounds of selection. (C) The sequences represent aptamers developed after 11 rounds of selection. A summary of the selection of the aptamer binding to thrombin at an epitope distinct from the binding site of the G15D aptamer.

Fig. 32 A diagram of methods for permanently linking the two aptamers recognizing two distinct epitopes of the target. (A) Two complimentary oligonucleotides are attached using linkers to each of the aptamers. These oligonucleotides are long enough (typically >15bps) to form a stable duplex permanently linking the two aptamers. (B) The two aptamers are connected directly via a linker.

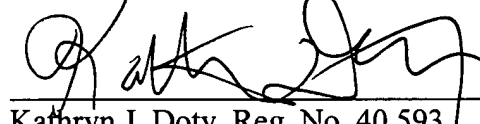
PATENT
Atty Docket No. 102364
Express Mail Label No. EV 535074245 US

Fig. 33 Example of a potential sensor design utilizing three sensing components. In this design the target is a complex of three components (light blue, dark blue, and black ovals). Each of the aptamers recognizes one of the components of the complex. Signals of different color from each of the two signaling oligonucleotide pairs could be used to discriminate between the entire complex containing all three components with alternative sub-complexes containing only two of the components.

Applicants' petition fee of \$130.00 is included in the enclosed check covering filing fees for this application. The Commissioner is hereby authorized to charge any additional fees which may be required as a result of this petition to Deposit Account No. 50-1662.

Respectfully submitted,

POLSINELLI SHALTON WELTE SUELTHAUS PC



Kathryn J. Doty, Reg. No. 40,593
100 South Fourth Street, Suite 1100
St. Louis, Missouri 63102
Tel: (314) 552-6850
Fax: (314) 231-1776
Attorney for Applicants

Date: June 15, 2005

048483 / 102364
KJDOT 289462